Submitted: 13 August, 2025 Accepted: 05 November, 2025 Published: 03 May, 2026 DOI:10.22514/jocpd.2026.074

ORIGINAL RESEARCH

Journal of Clinical Pediatric Dentistry

Evaluation of the biomechanical effects of pediatric crowns applied to endodontically treated primary molars: a three-dimensional finite element analysis

Merve Taşcı Dedeoğlu[1], Merve Abaklı İnci[1,*]

[1]Department of Pediatric Dentistry, Faculty of Dentistry, Necmettin Erbakan University, 42090 Konya, Türkiye

***Correspondence**
mabakli@erbakan.edu.tr
(Merve Abaklı İnci)

Abstract

Background: The choice of crown material following endodontic treatment in primary molars is critical for biocompatibility and long-term clinical success. This study aimed to compare the stress distribution patterns caused by stainless steel crowns (SSC), pediatric zirconia crowns (PZC), and Bioflx crowns—placed on pulpotomized primary molars—in combination with different luting cements, under maximum bite force using three-dimensional finite element analysis (3D-FEA). **Methods**: A 3D model of a caries-free, anatomically intact maxillary primary molar was created from micro-computed tomography (micro-CT) images. A virtual pulpotomy was simulated using mineral trioxide aggregate (MTA) and conventional glass ionomer cement (GIC). SSC, PZC, and Bioflx crowns were modeled in various combinations with either GIC or resin-modified glass ionomer cement (RMGIC). Based on the mechanical properties reported in the literature, a total load of 245 N was applied at angles of 0°, 45°, and 90°, and stress distributions and maximum von Mises stress values were evaluated in the luting cement layer, dentin, and pulp tissues. **Results**: In the Bioflx crown models, von Mises stress values in both the dentin and cement layers were higher compared with those in the SSC and PZC models. The lowest stress values were observed in the PZC models. Stress levels within the radicular pulp were similar across all models and remained below the thresholds for biological damage. The healthy tooth model showed intermediate stress values between those of the SSC and PZC models. Models utilizing RMGIC exhibited lower stress levels in the cement layer but higher stress in dentin and pulp; however, these differences did not represent a relevant variation. **Conclusions**: The findings indicate that the directionally applied 245 N masticatory force has a direct impact on the biomechanical performance of both the crown material and the luting cement. Notably, the Bioflx crown models' elevated stress levels indicate that a thorough clinical assessment is necessary before using it.

Keywords

Pulpotomy; Pediatric dentistry; Crown; Finite element analysis; Glass ionomer cement; Resin-modified glass ionomer cement; Molar

1. Introduction

Primary teeth's unique morphology, characterized by thinner enamel and dentin, contributes to rapid caries progression and challenges in pediatric dentistry [1]. Pulpotomy is a widely used treatment procedure that aims to remove the coronal pulp while preserving the vitality of the radicular pulp [2]. After this treatment, the prompt placement of a durable and leakage-free restoration is crucial for preserving the functional integrity of the tooth and ensuring long-term success of the therapy [3].

In this context, full-coverage pediatric crowns are widely employed. Stainless steel crowns (SSCs), which have been routinely preferred since the 1950s, are long-standing restorations valued for their high durability and retention in primary teeth. Because they are straightforward to place, cost-effective, and demonstrate favorable long-term outcomes, SSCs remain a common choice. However, their metallic appearance may not satisfy aesthetic expectations and can reduce patient and parent satisfaction, particularly when aesthetics are a priority [4, 5]. To overcome these aesthetic shortcomings, pediatric zirconia crowns (PZC) have been developed as prefabricated, ceramic-based restorations that meet both functional and aesthetic demands. These zirconia dioxide-based crowns are preferred for their tooth-like opacity, excellent biocompatibility, and smooth surfaces that reduce plaque accumulation [6–8]. However, compared with SSCs, PZCs require more precise tooth preparation for proper intraoral fit, which increases the need for technical sensitivity during application.

Recently, Bioflx crowns have emerged as a new generation of crown materials, drawing attention due to their aesthetic and flexible nature. This hybrid polymer-based material aims to combine the retention advantages of SSCs with the aesthetics of PZCs. Thanks to its flexibility, Bioflx can provide a more comfortable adaptation to the tooth and demonstrate resistance to masticatory forces due to its high impact strength. Moreover, Bioflx crowns offer micromechanical retention on the tooth surface, which facilitates the cementation process, shortens the clinical application time, and reduces the need for recementation [9–11].

Biomechanical analysis methods play a significant role in evaluating the clinical performance of these materials. In particular, Finite Element Analysis (FEA) is a powerful engineering tool that allows for the quantitative assessment of stress and deformation in complex dental structures. Through computer-aided simulations, FEA provides data on stress distribution that would be difficult to obtain in *in vivo* studies. By modeling real anatomical structures, the biomechanical behavior of various crown and cement combinations can be comparatively analyzed under controlled conditions on three-dimensional (3D) digital models. As a result, the potential effects of restorative materials on dental tissues can be predicted, offering a scientific basis for clinical decision-making [12, 13].

This study aims to comparatively evaluate the stress distribution that occurs following the cementation of SSCs, PZCs, and Bioflx crowns on pulpotomized primary molars using GIC or RMGIC, by means of 3D-FEA. The main innovation of the study is the finite element evaluation of Bioflx crowns, for which clinical and biomechanical evidence is limited. However, SSCs and PZCs were included as established comparators to provide meaningful clinical context and highlight the relative performance of Bioflx crowns. The findings are expected to provide scientific guidance for material selection in pediatric restorative treatments, particularly for newer crown materials.

2. Materials and methods

2.1 Study design and acquisition of micro-CT images

This study was designed to evaluate the biomechanical effects of different pediatric crown materials in endodontically treated primary molars. A caries-free, unrestored, and anatomically intact maxillary second primary molar—extracted for therapeutic purposes—was obtained from the Department of Pediatric Dentistry, Faculty of Dentistry, Necmettin Erbakan University. In this study, primary maxillary second molars were selected because they play a critical role in preserving arch length and preventing mesiopalatal rotation of the permanent first molars, and they are among the most frequently treated teeth in pediatric restorative dentistry. The tooth was sent to the Research Laboratory of the Faculty of Dentistry at Erciyes University for micro-CT scanning. Scanning was performed using a Bruker Skyscan 1272 system (Karlsruhe, BW, Germany) at 75 kV and 133 μA, with a voxel size of 21.758200 μm.

2.2 Finite element stress analysis process and mesh generation

The design of the 3D mesh structure, the mathematical transformation of the solid model into an analyzable form, its adaptation for finite element analysis, and the execution of stress analyses were all performed using HP workstations equipped with Intel Xeon E-2286 processors (2.40 GHz, Intel Corporation, Santa Clara, CA, USA) and 64 GB Error-Correcting Code (ECC) memory.

The tooth model was generated from tomographic data using 3D Slicer software (Fig. 1). This platform was used for both volumetric segmentation and Standard Tessellation Language (STL)-format export. The resulting data were converted into 3D solid models using a reverse engineering approach in ANSYS SpaceClaim (version 2021 R2, ANSYS Inc., Canonsburg, PA, USA). Adaptation of the solid models for analysis, mesh generation, and the application of loading conditions were carried out in ANSYS Workbench (ANSYS Inc., Canonsburg, PA, USA).

The finite element analysis computations were performed using the LS-DYNA solver (version not specified, Livermore Software Technology Corporation, Livermore, CA, USA).

2.3 Model preparation

The dentin and enamel structures obtained from the tomography data were imported into ANSYS SpaceClaim software (ANSYS Inc., Canonsburg, PA, USA) and converted into 3D solid models. A structure extending from the pulp chamber to the root canals was created within the dentin tissue, and a 2 mm-high MTA model (MTA, Dentsply Tulsa Dental Specialties, OK, USA) was designed. The remaining pulp space was filled with conventional glass ionomer cement (GIC) (GC Fuji II®, Gold Label, GC Corporation, Tokyo, Japan), thereby completing the virtual pulpotomy procedure (Fig. 2). It should be noted that the MTA was incorporated solely to simulate the pulpotomy procedure and to preserve the anatomical fidelity of the restored tooth model. However, MTA was not the primary focus of this study. The main objective was to evaluate the biomechanical behavior of different crown-cement combinations, and the inclusion of MTA served only to establish a realistic clinical baseline for the analysis.

Virtual tooth preparations were performed on the base tooth model according to the following dimensions for three different crown types: Stainless Steel Crown (SSC) (3M ESPE, MN, USA): 1.5 mm occlusal reduction, 1 mm proximal reduction; Bioflx Crown (Kids-e-dental, LLP, India): 1.5 mm occlusal reduction, 0.5 mm proximal reduction; Pediatric Zirconia Crown (PZC) (Ez-Pedo, Loomis, California, USA): 2 mm occlusal reduction, 1 mm proximal reduction (Fig. 3).

On each preparation model, adhesive cement layers were modeled at a uniform thickness of 0.2 mm, referencing the outer surface, using either conventional GIC (GC Fuji I®, GC Corporation, Tokyo, Japan) or resin-modified glass ionomer cement (RMGIC) (GC FujiCEM® 2, GC Corporation, Tokyo, Japan) (Fig. 4) [14]. Restorative crown materials were then defined over the adhesive layer with the following standard thicknesses [15]. Bioflx crown: 0.13 mm; Stainless steel crown: 0.13 mm; Pediatric zirconia crown: 0.73 mm.

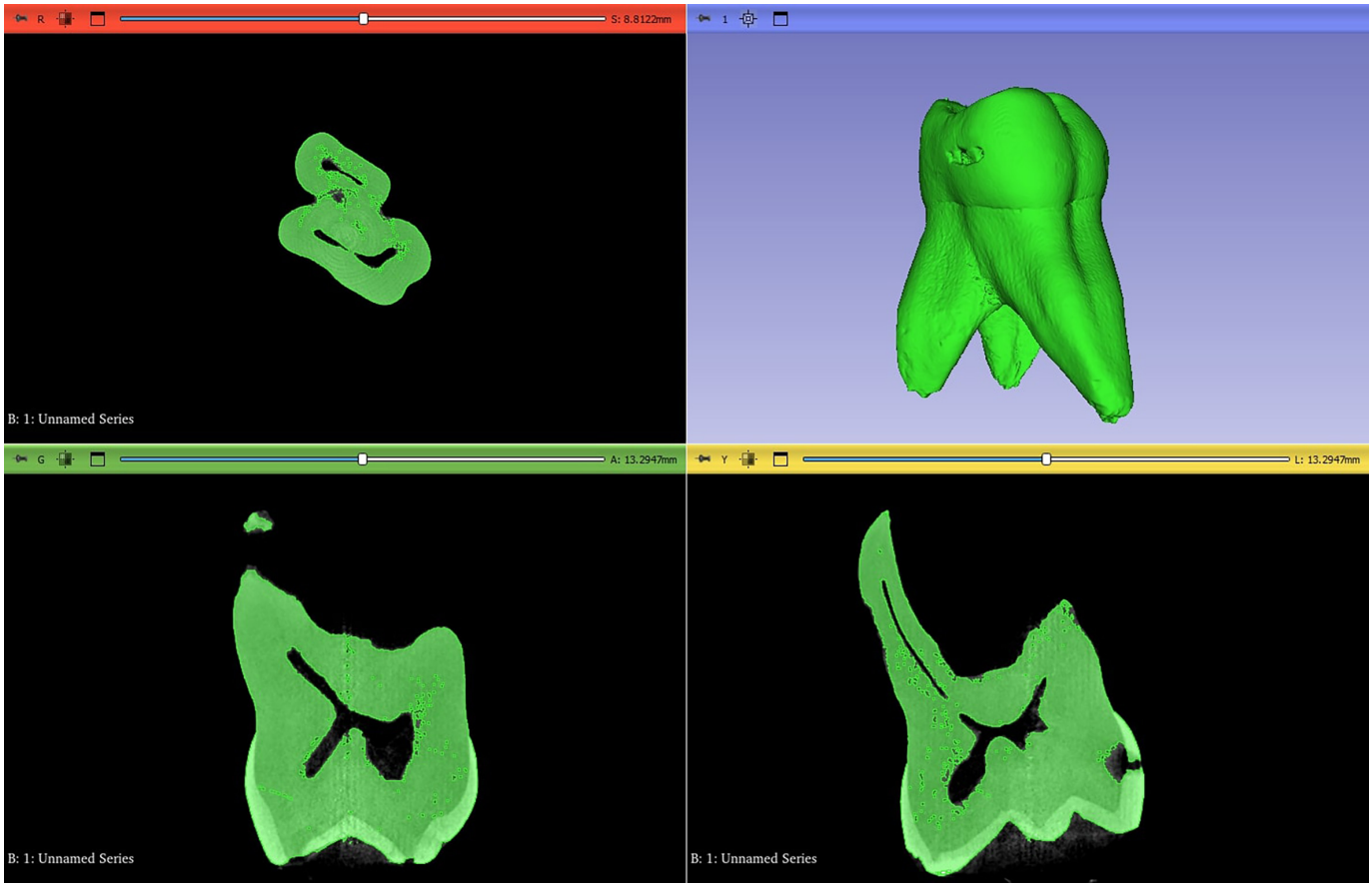

FIGURE 1. Visualization of the tomography data obtained after reconstruction.

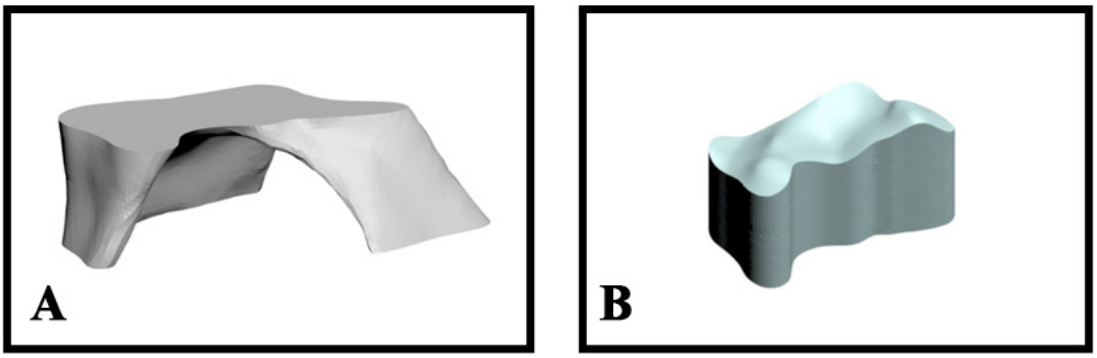

FIGURE 2. Three-dimensional models of the materials used in the pulpotomy simulation. (A) Three-dimensional model of mineral trioxide aggregate (MTA). (B) Three-dimensional model of glass ionomer cement (GIC).

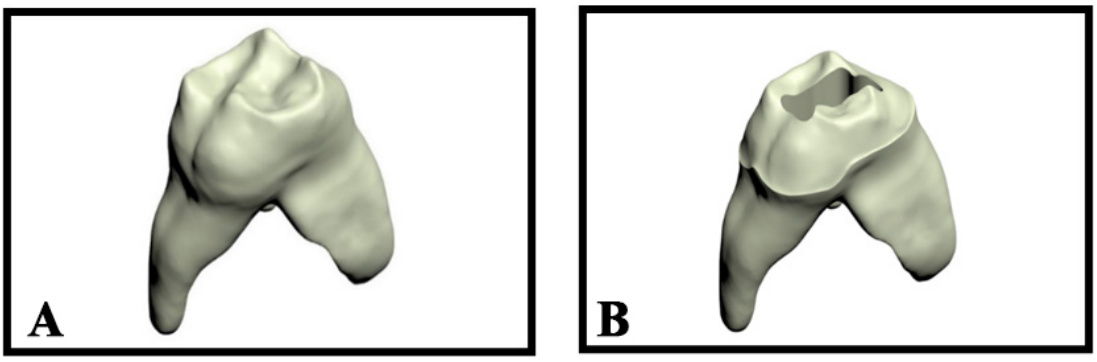

FIGURE 3. Dentin structure in healthy and crown-prepared tooth models. (A) Dentin structure in the healthy tooth model. (B) Dentin structure in the crown-prepared tooth model.

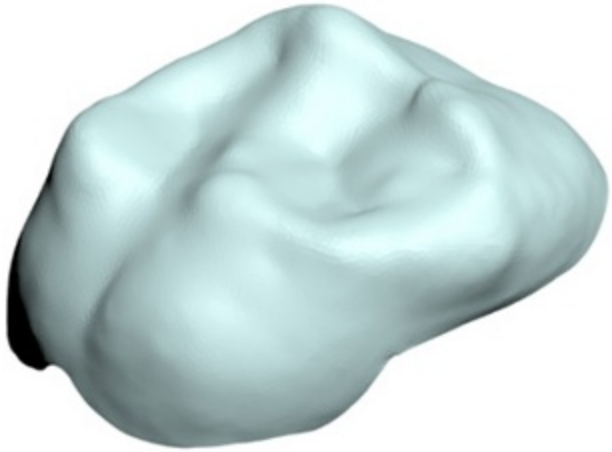

FIGURE 4. 3D modeling of glass ionomer cement and resin-modified glass ionomer cement to be used when bonding the crown material.

At the junction of the tooth and crown structures, a periodontal ligament (PDL) layer with a uniform thickness of 0.25 mm was modeled, using the outer surface of the dentin as a reference (Fig. 5). This PDL layer was incorporated into the system to simulate the biomechanical behavior accurately [16].

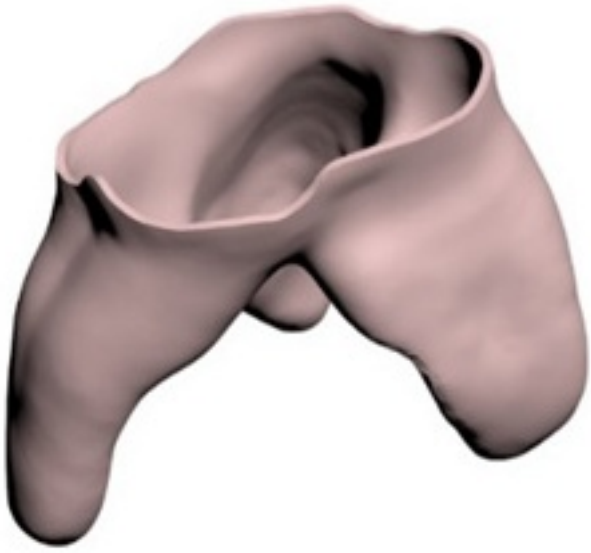

FIGURE 5. Creation of periodontal ligament design.

These crowns were combined with two different luting cements (GIC and RMGIC), resulting in a total of six experimental models. Additionally, a healthy tooth model was included as a control group (Table 1).

The alveolar bone was not obtained from the micro-CT images of the extracted tooth. Instead, the maxillary bone model was reconstructed from CT data of the Visible Human Project, with a slice thickness of 0.33 mm. Cortical and trabecular bone were segmented in 3D Slicer based on Hounsfield unit thresholds and exported in STL format. The cortical bone was modeled with a uniform thickness of approximately 2 mm surrounding the trabecular bone, which extended from the cemento-enamel junction to the apical region of the roots.

TABLE 1. Study models.

Model	Model Description
Model 1	Bioflx Crown—GIC
Model 2	Bioflx Crown—RMGIC
Model 3	Stainless Steel Crown—GIC
Model 4	Stainless Steel Crown—RMGIC
Model 5	Pediatric Zirconia Crown—GIC
Model 6	Pediatric Zirconia Crown—RMGIC
Control Model	Healthy Tooth Model

GIC: glass ionomer cement; RMGIC: resin-modified glass ionomer cement.

The material properties (elastic modulus and Poisson's ratio) of both cortical and trabecular bone were defined according to the literature (Table 2).

2.4 Mesh generation and analysis process

The geometric models were transformed into mathematical models by dividing them into small and simple elements known as "meshes". Following the completion of 3D modeling in ANSYS SpaceClaim, the data were transferred to the ANSYS Workbench platform for analysis preparation.

All models were meshed using highly refined triangular (tria) surface elements with a size range of 0.1–0.25 mm. The solid structures were meshed using tetrahedral (four-faced) elements. These meshing parameters were selected based on previously published finite element studies in dental biomechanics, which reported that such mesh designs provide sufficient accuracy for modeling complex tooth geometries [17, 18]. A separate convergence analysis was not performed in this study; however, the selected mesh density has been validated in the literature as adequate for reliable stress distribution analysis.

These mathematical models were then transferred to the LS-DYNA solver for finite element analysis.

2.5 Material properties

All materials were assumed to exhibit linear elastic, homogeneous, and isotropic behavior. The values for elastic modulus and Poisson's ratio were assigned based on relevant literature sources [19–24].

2.6 Loading scenarios and boundary conditions

A total force of 245 N was applied in all models at 45° and 90° angles directed toward the palatal slope of the buccal cusp, and at a 0° vertical angle from the central fossa.

In this study, 3D models of maxillary second primary molars restored with different crown and cement combinations following MTA pulpotomy were analyzed using finite element analysis under a load of 245 N applied from three different directions. The forces were applied at vertical (0°) (Fig. 6), oblique (45°) (Fig. 7), and horizontal (90°) (Fig. 8) angles, and the resulting stress distributions were evaluated based on

TABLE 2. Elastic modulus and Poisson's ratio values of the analyzed models.

Material	Elastic Modulus (MPa)	Poisson's Ratio
Enamel	80,350	0.33
Dentin	19,890	0.31
Pulp	2000	0.45
Trabecular Bone	490	0.30
Cortical Bone	14,700	0.30
Luting Glass Ionomer Cement (GIC)	10,800	0.30
Resin-Modified Glass Ionomer Cement	4920	0.27
Base Glass Ionomer Cement	12,000	0.30
Stainless Steel Crown	200,000	0.33
Pediatric Zirconia Crown	242,000	0.26
Bioflx Crown	5030	0.39
Periodontal Ligament	69	0.45
Mineral Trioxide Aggregate (MTA)	11,760	0.31

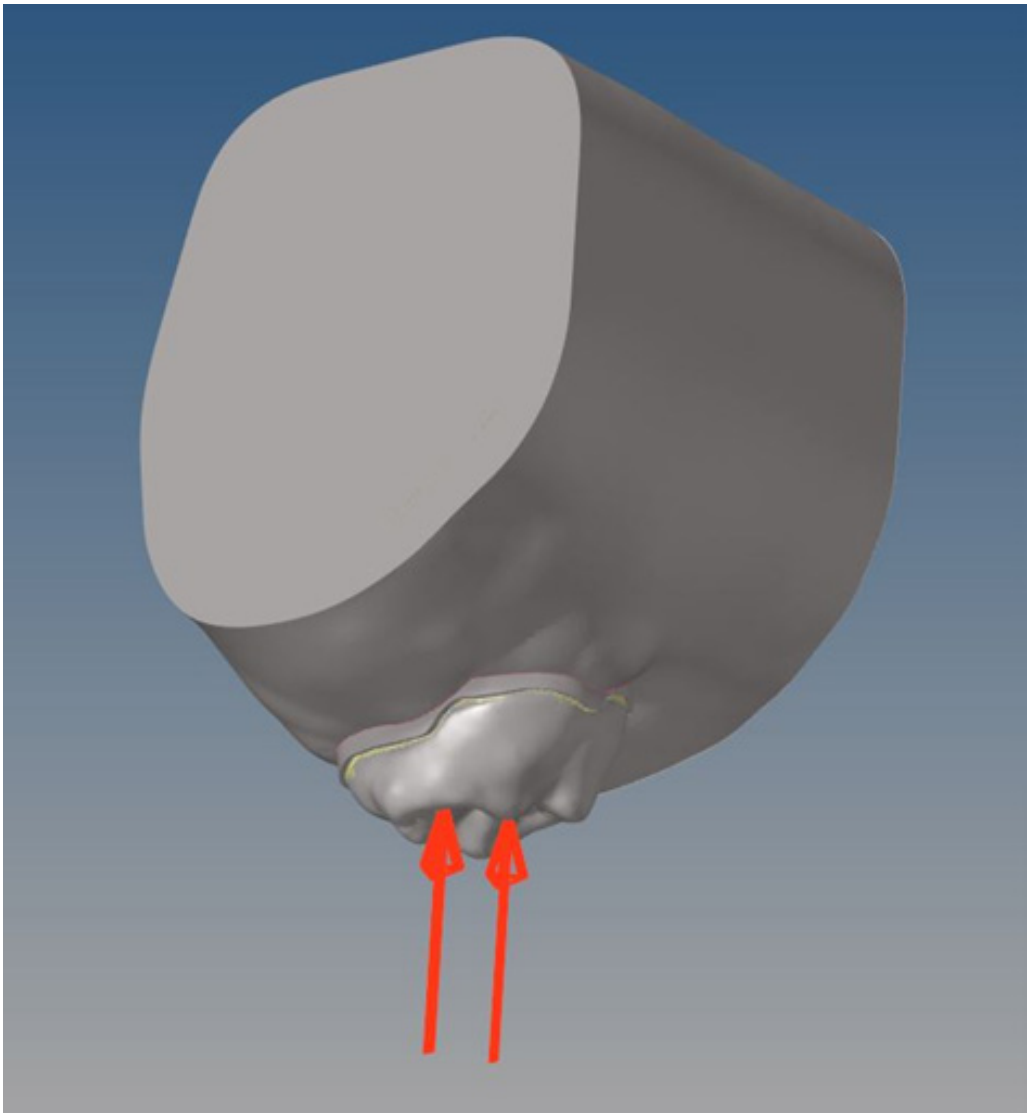

FIGURE 6. Location and direction of force application. Application of a total vertical force of 245 N at a 0° angle from the central fossa.

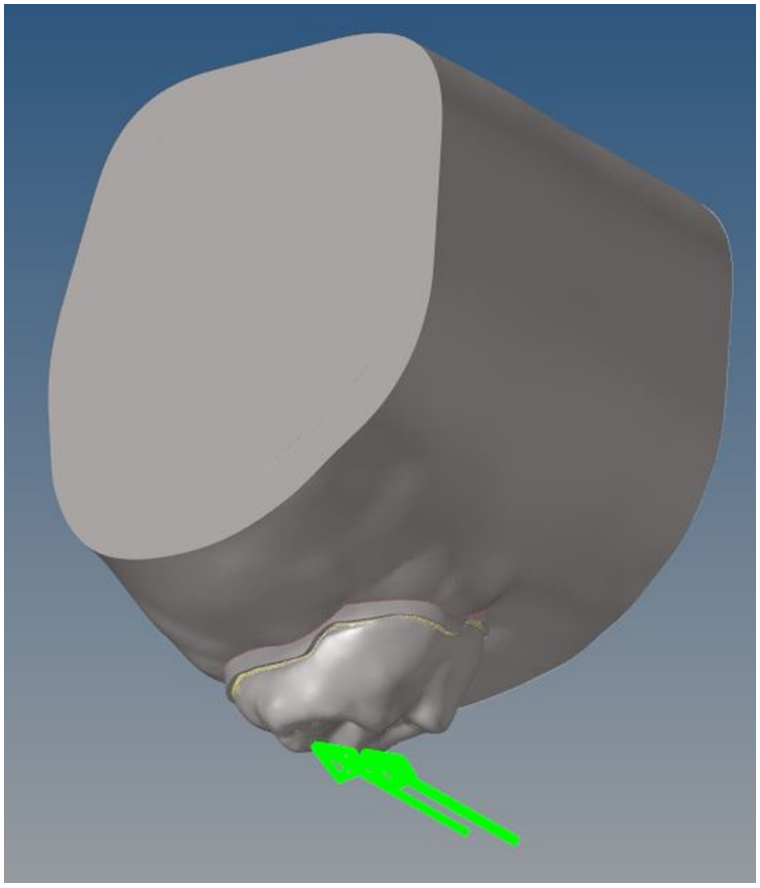

FIGURE 7. Location and direction of force application. Application of a total oblique force of 245 N at a 45° angle toward the palatal slope of the buccal cusp.

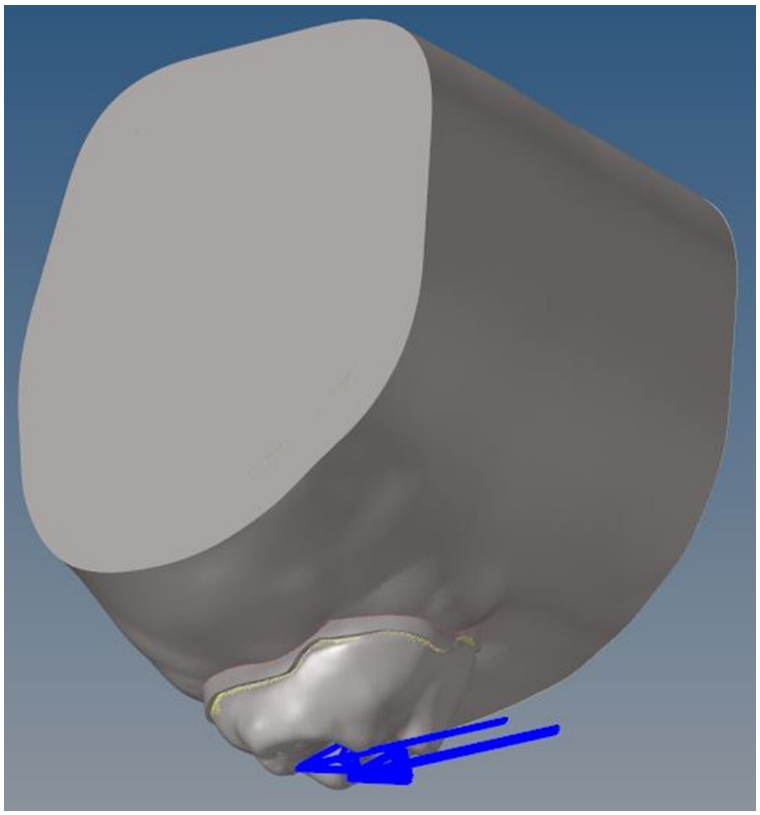

FIGURE 8. Location and direction of force application. Application of a total horizontal force of 245 N at a 90° angle toward the palatal slope of the buccal cusp.

the maximum von Mises stress values observed in the adhesive cement, dentin, and pulp tissues.

Previous studies have reported that the maximum bite force in primary and mixed dentition ranges between 161 and 330 N [25, 26]. For instance, a clinical study involving 8-year-old children in mixed dentition reported a maximum bite force of 289.23 N [27]. Accordingly, a load of 245 N was applied in the present study to simulate functional masticatory forces.

To prevent stress singularities in the loading regions, the forces were distributed across the surrounding nodal points. The bone models were fixed in all three axes, and all surface contacts were defined as "bonded".

In the analysis stage, the evaluation criteria included the stress distributions and maximum von Mises stress values in luting cement layer, dentin, and pulp tissues. These parameters were assessed under vertical (0°), oblique (45°), and horizontal (90°) loading conditions to comprehensively evaluate the biomechanical performance of the different crown-cement combinations.

2.7 Quantitative model information

In this study, a high mesh density was employed, with the number of nodes ranging from 429,170 to 441,718 and the number of elements ranging from 1,690,054 to 1,753,684, thereby enhancing the precision of the finite element model and providing results that more closely reflect clinical conditions (Table 3).

TABLE 3. Quantitative information of the created models.

Models	Total # of Nodes	Total # of Elements
Model 1	441,718	1,720,443
Model 2	441,718	1,720,443
Model 3	439,125	1,711,269
Model 4	439,125	1,711,269
Model 5	429,170	1,690,054
Model 6	429,170	1,690,054
Control Model	440,546	1,753,684

However, no experimental or clinical validation of the finite element models was performed; therefore, the stress values obtained in this study should be regarded as theoretical estimations rather than absolute clinical outcomes.

2.8 System integration and contact definitions

For the mathematical models to be constructed and to obtain accurate results, it was necessary to define the contact surfaces between the components in the analysis software. Therefore, "bonded" contact definitions were applied to the interacting regions of all models. In addition, before proceeding to the meshing stage, an interference check was performed in ANSYS SpaceClaim for all assemblies to ensure that no overlapping geometries or mismatched contacts existed between the crown, luting cement, tooth structures, periodontal ligament, and bone. This approach assumed that the components moved in complete correlation during loading.

3. Results

3.1 Findings under vertical force (0°)

When a vertical force was applied at a 0° angle along the long axis of the tooth, higher stress values were observed in GIC groups compared with RMGIC groups across all crown models in the adhesive cement layer. The highest stress in dentin was recorded in the Bioflx crown model (335.16 MPa), while the lowest was in the PZC + GIC model (18.48 MPa). In the pulp tissue, the highest von Mises stress was observed in the healthy tooth model.

3.2 Findings under oblique force (45°)

When an oblique force was applied at a 45° angle, all crown models with RMGIC showed lower stress values in the adhesive cement compared with those with GIC. The lowest stress values in dentin were observed in models restored with PZC (33.28 MPa and 37.86 MPa). In the pulp tissue, the von Mises stress values in all restored models were lower than those observed in the pulp of the healthy tooth model.

3.3 Findings under horizontal force (90°)

When a horizontal force was applied at a 90° angle, the highest stress in the adhesive cement was recorded in the Bioflx + GIC model (499.68 MPa), while the lowest was found in the PZC + RMGIC model (8.70 MPa). In the dentin, the Bioflx + RMGIC combination exhibited higher stress compared with other groups (419.69 MPa). In the pulp tissue, the highest von Mises stress was observed in the healthy tooth model (2.88 MPa), whereas the restored models showed lower and relatively similar values.

3.4 Stress distribution comparison by force angle

3.4.1 Adhesive cements

When comparing stress values in the adhesive cement layers under different force angles, it was observed that as the force angle increased, the stress levels decreased across all models (Fig. 9).

3.4.2 Dentin tissue

The maximum stress values in the dentin increased with the force angle in models restored with Bioflx and PZC, whereas a decrease was observed in models with SSC (Fig. 10).

For greater clarity, we included stress distribution plots of the most critical models (horizontal loading at 90°), which displayed dentin stresses with a standardized color scale legend, and we compared these values with those of the sound tooth model to better demonstrate the biomechanical differences among the evaluated crown-cement combinations (Figs. 11,12).

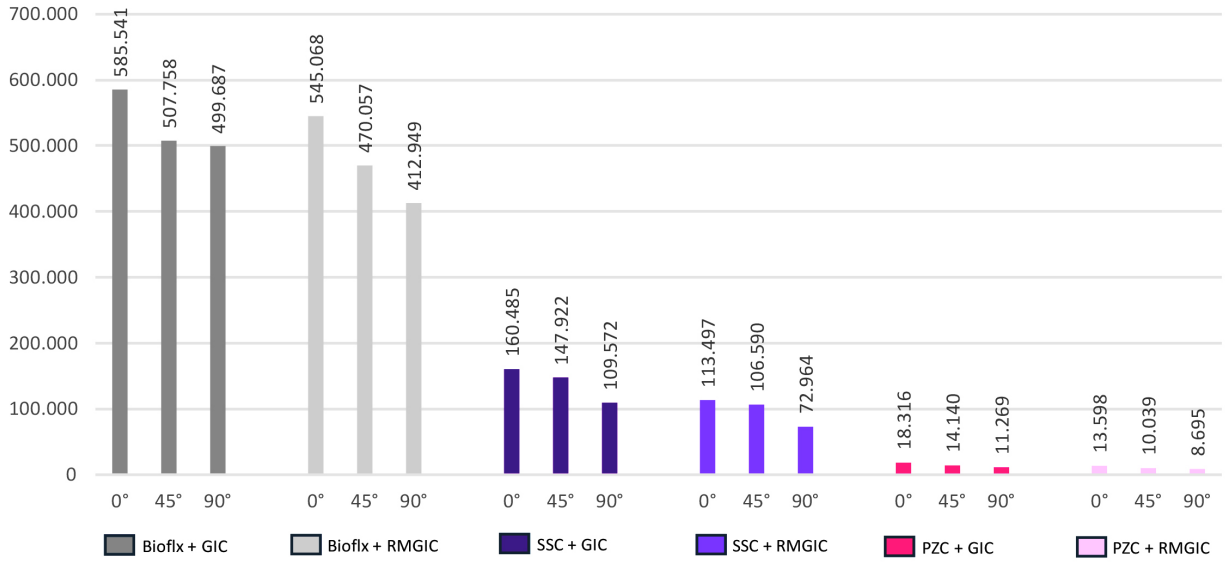

FIGURE 9. Maximum von Mises stress values in the adhesive cements under different loading conditions. GIC: glass ionomer cement; RMGIC: resin-modified glass ionomer cement; SSC: stainless steel crowns; PZC: pediatric zirconia crowns.

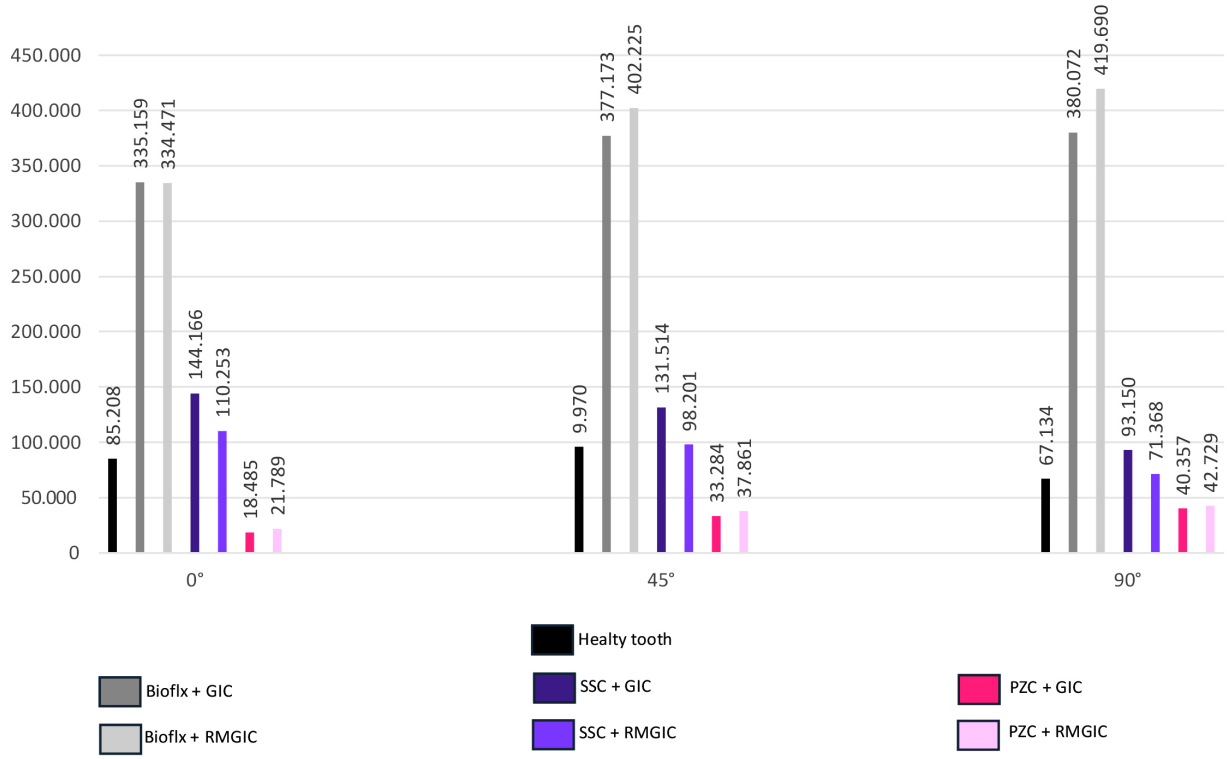

FIGURE 10. Maximum von Mises stress values in the dentin tissue under different loading conditions. GIC: glass ionomer cement; RMGIC: resin-modified glass ionomer cement; SSC: stainless steel crowns; PZC: pediatric zirconia crowns.

3.4.3 Pulp tissue

The maximum stress values observed in the pulp tissue under different force angles were found to be relatively similar across all models (Fig. 13).

4. Discussion

In this study, three-dimensional finite element stress analysis (3D-FEA) was employed to evaluate the stress distribution patterns created by different crown and cement combinations on an endodontically treated second primary molar under three different directional forces. The results demonstrated that the mechanical properties of the restorative materials exert a substantial influence on biomechanical behavior.

In crowned tooth models, the anatomical complexity and layered morphology of the crown often limit the precision of classical methods used to define surface contours. As a result, tooth geometry is frequently simplified or reduced to two-dimensional representations, which may compromise the reliability of accurately analyzing mechanical behavior [28].

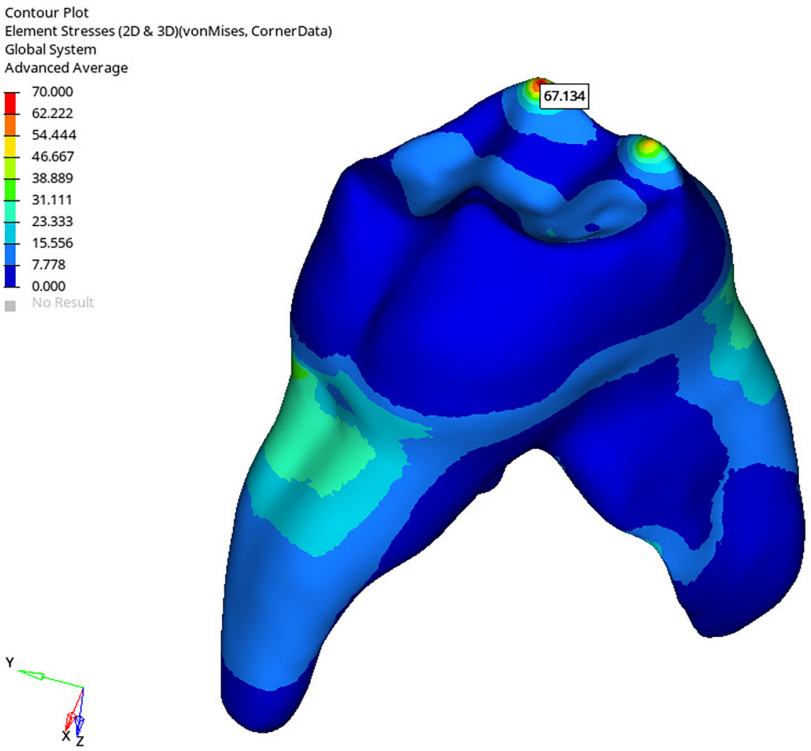

FIGURE 11. Distribution of stresses occurring in the dentin after applying horizontal force at a 90° angle to the long axis of the tooth on a healthy tooth model.

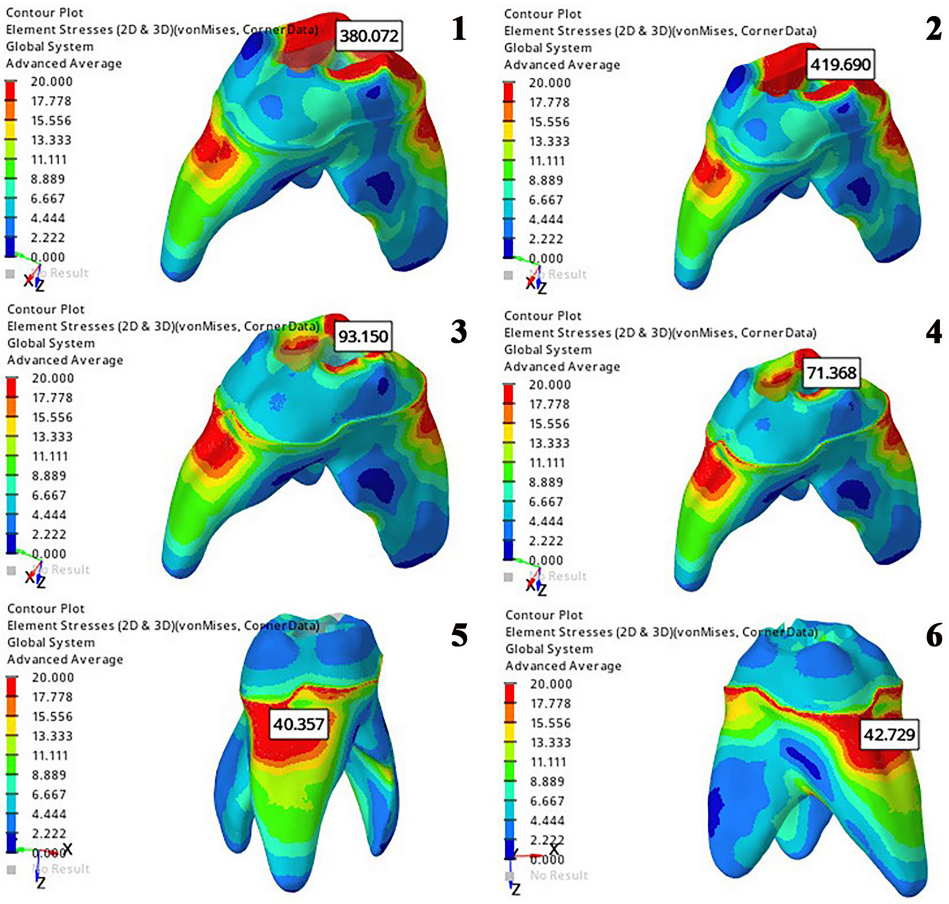

FIGURE 12. Stress distributions on the dentin tissue after applying a horizontal force at a 90° angle to the long axis of the tooth in the study models (Models 1,2,3,4,5,6 from left to right, respectively).

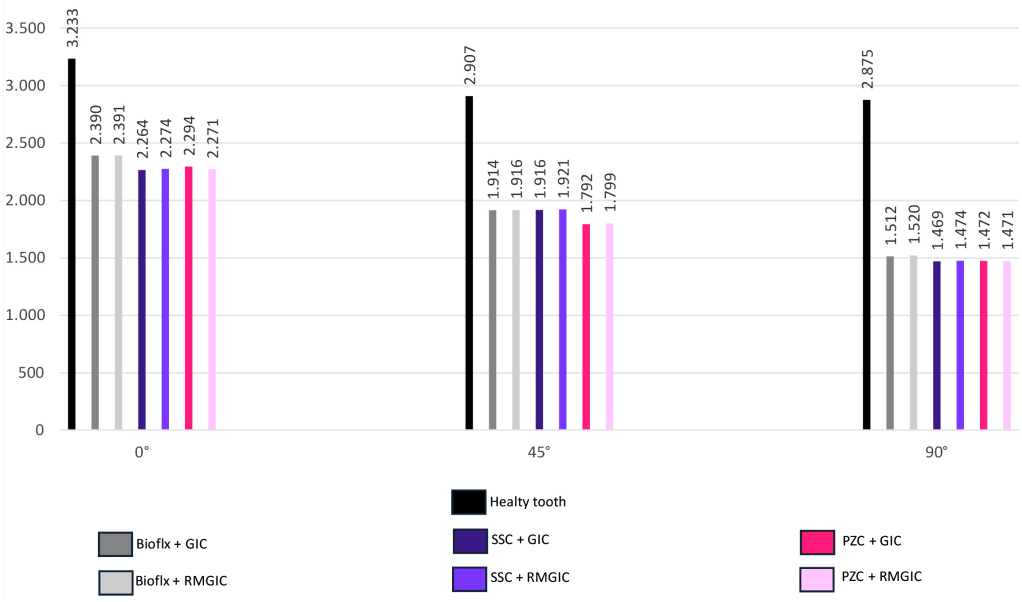

FIGURE 13. Maximum von Mises stress values measured in the pulp tissue under different loading conditions. GIC: glass ionomer cement; RMGIC: resin-modified glass ionomer cement; SSC: stainless steel crowns; PZC: pediatric zirconia crowns.

In light of these constraints, the structures in the present finite element models were assumed to be linear, isotropic, and homogeneous, which should be acknowledged as a limitation of this study.

The thickness and type of cement used in cementing crowns affect the stress distribution in different layers of the tooth. Based on evidence from previous studies and manufacturers' recommendations, a luting thickness of 0.2 mm was used for the cementation of SSC, PZC, and Bioflx crowns in this study, employing either glass ionomer cement (GIC) or resin-modified glass ionomer cement (RMGIC) [27, 29]. In the comparison between conventional GIC and RMGIC, GIC was found to absorb more stress due to its higher elastic modulus, whereas RMGIC distributed the load more uniformly due to its more flexible nature [30, 31]. These findings are consistent with previous studies reporting that cements with higher elastic moduli tend to result in greater stress concentrations within the luting layer [32, 33].

The findings also revealed that different crown-cement combinations play a decisive role in the distribution of stress values. Particularly in the models restored with Bioflx crowns, von Mises stresses were higher in both the dental tissues and the adhesive cement compared with other materials. This may be attributed to the lower elastic modulus and viscoelastic nature of the Bioflx material. More flexible materials are thought to absorb less applied force and transmit more stress to deeper tissues, such as dentin and pulp. Similar findings in the literature support this; for instance, Ruck and Gosnell reported that Bioflx undergoes greater deformation under lateral loads, potentially compromising restoration success [11].

Pediatric zirconia crowns emerged as the material with the lowest stress transmission. Owing to zirconia's high elastic modulus, a substantial portion of the applied load was absorbed, reducing stress transmission to the dental tissues. This finding aligns with studies by Prabhakar *et al.* [34], who reported that zirconia crowns reduce dentinal stress. Considering zirconia's biocompatibility and aesthetic advantages, it remains a highly favorable option for use in pediatric patients.

Stainless steel crowns were found to transmit a moderate level of stress. These restorations have long been used in pediatric dentistry and are known for their durability. Previous studies have emphasized the clinical success of stainless steel crowns, noting their ability to withstand functional loads, especially in posterior regions [35, 36].

The direction of the applied force also had a direct influence on stress distribution. Under oblique and horizontal forces, increased dentinal stress was particularly evident in the Bioflx and PZC groups. This highlights the importance of selecting restorative materials capable of withstanding not only vertical but also lateral masticatory forces in clinical settings. Other studies have similarly emphasized the effect of force direction on the performance of restorative materials [37, 38]. In previous studies, lateral masticatory forces have been simulated at 0°, 45°, and 90° by applying angled loads to the palatal slopes of the buccal cusps [24, 26]. In line with this approach, our study adopted these load directions to reflect clinically relevant scenarios, where vertical forces (0°) represent normal mastication, oblique forces (45°) functional contacts during chewing, and horizontal forces (90°) parafunctional loading such as bruxism.

The stress values observed in the pulp tissue across all groups remained below the biologically acceptable thresholds reported in the literature. According to Tanaka *et al.* [39], stresses exceeding 2.94–3 MPa may be harmful to the pulp, whereas the values observed in this study were within the safe range.

The FEA method is widely regarded as a reliable approach for evaluating the biomechanical behavior of restorative materials [40, 41]. In the present study, modeling of Digital Imaging and Communications in Medicine (DICOM) format-

ted micro-CT scans via 3D Slicer enabled the reconstruction of geometries closely resembling clinical anatomy [42]. The use of a high number of nodes and elements (approximately 440,000 nodes and 1.7 million elements) further enhanced the precision of the analysis [43].

Despite these methodological strengths, the main limitation of the present study is the absence of experimental or clinical validation of the finite element models. While finite element analysis provides valuable insights into biomechanical behavior, the absolute stress values reported herein should be considered theoretical approximations. Moreover, the stress differences observed in this study do not directly translate into clinical failure. Real-world factors, such as the need for crown reshaping, marginal adaptation, indication restrictions (*e.g.*, limited space, esthetic concerns, or remaining tooth structure), wear, cement dissolution, occlusal adjustments, and individual chewing patterns, were not modeled. Therefore, the findings should be interpreted as indicative of potential mechanical tendencies rather than definitive clinical predictions. Future studies incorporating sensitivity analyses, strain-gauge comparisons, or clinical validation are required to further substantiate the reliability and translational relevance of these findings. Future studies should incorporate dynamic loading simulations, thermomechanical cycling, and in vitro testing of extracted teeth to validate the finite element findings.

5. Conclusions

This study evaluated the biomechanical behavior of maxillary second primary molars restored with different crown-cement combinations following MTA pulpotomy by using finite element analysis. The results showed that pediatric zirconia crowns produced the lowest von Mises stress values in the dentin and cement layers, indicating favorable stress distribution. Stainless steel crowns demonstrated moderate stress levels, while Bioflx crowns exhibited higher stress concentrations under horizontal loading. Within the limitations of this simulation-based study, these findings provide comparative biomechanical data that may guide the selection of pediatric full-coverage crowns in clinical practice.

AVAILABILITY OF DATA AND MATERIALS

The data that support the findings of this study are available from the corresponding author upon reasonable request.

AUTHOR CONTRIBUTIONS

MTD—Study design, implementation of finite element modeling, data analysis, literature review, manuscript writing. MAİ—Study design, scientific supervision, interpretation of findings, scientific and linguistic revision of the manuscript. Both authors contributed to editorial changes in the manuscript. Both authors read and approved the final manuscript.

ETHICS APPROVAL AND CONSENT TO PARTICIPATE

Ethical approval for this study was obtained from the Non-Pharmaceutical and Non-Medical Device Research Ethics Committee of Necmettin Erbakan University Faculty of Dentistry on 28 March 2024, under decision number 2024/390. As this finite element analysis study was based solely on computational simulations and contained no human participants, patient data informed consent is not applicable.

ACKNOWLEDGMENT

Not applicable.

FUNDING

This study was supported by the Scientific Research Projects Unit of Konya Necmettin Erbakan University under project number 24DU2404.

CONFLICT OF INTEREST

The authors declare no conflict of interest.

REFERENCES

[1] Bogovska-Gigova R, Hristov K. Quantitative assessment of enamel and dentin volumes in primary teeth using micro-computed tomography. Journal of IMAB. 2025; 31: 6380–6385.

[2] Coll JA, Dhar V, Chen CY, Crystal YO, Guelmann M, Marghalani AA, *et al.* Use of vital pulp therapies in primary teeth 2024. Pediatric Dentistry. 2024; 46: 13–26.

[3] Lai G, Sheng K, Zhao J, Ding N, Zhao S, Wang J. A retrospective study on the outcome of pulpotomy with iRoot BP plus in primary molars and its relationship with hemostasis time. BMC Oral Health. 2024; 24: 1134.

[4] Amlani DV, Brizuela M. Stainless steel crowns in primary dentition. StatPearls Publishing: Treasure Island (FL). 2023.

[5] Pei SL, Chen MH. Comparison of periodontal health of primary teeth restored with zirconia and stainless steel crowns: a systemic review and meta-analysis. Journal of the Formosan Medical Association. 2023; 122: 148–156.

[6] Diener V, Polychronis G, Erb J, Zinelis S, Eliades T. Surface, microstructural, and mechanical characterization of prefabricated pediatric zirconia crowns. Materials. 2019; 12: 3280.

[7] Khatri A. Esthetic zirconia crown in pedodontics. International Journal of Pedodontic Rehabilitation. 2017; 2: 31–33.

[8] Rahate I, Fulzele P, Thosar N. Comparative evaluation of clinical performance, child and parental satisfaction of Bioflx, zirconia and stainless steel crowns in pediatric patients. F1000Research. 2023; 12: 756.

[9] Goswami M, Jangra B, Chauhan N, Khokhar A. Esthetics in pediatric dentistry—BioFlx crowns: case series. International Journal of Clinical Pediatric Dentistry. 2024; 17: 357.

[10] Patil AS, Jain M, Choubey S, Patil M, Chunawala Y. Comparative evaluation of clinical success of stainless steel and Bioflx crowns in primary molar—a 12 month split mouth prospective randomized clinical trial. Journal of Indian Society of Pedodontics and Preventive Dentistry. 2024; 42: 37–45.

[11] Ruck P, Gosnell ES. Selecting an esthetic full coverage restorative material for high caries-risk primary molars. Journal of Dentistry for Children. 2023; 90: 173–177.

[12] Chun HJ, Cheong SY, Han JH, Heo SJ, Chung JP, Rhyu IC, *et al.* Evaluation of design parameters of osseointegrated dental implants using

finite element analysis. Journal of Oral Rehabilitation. 2002; 29: 565–574.
[13] Ramoğlu S, Ozan O. Finite element methods in dentistry. Journal of the Faculty of Dentistry, Atatürk University. 2014; 9: 175–180.
[14] Waly AS, Souror YR, Yousief SA, Alqahtani WM, El-Anwar MI. Pediatric stainless-steel crown cementation finite element study. European Journal of Dentistry. 2021; 15: 77–83.
[15] Christensen GJ. Pediatric crowns are growing up. Clinicians Report. 2012; 5: 3–4.
[16] Abuelenain DA, Ajaj R, El-Bab EIF, Hammouda MM. Comparison of stresses generated within the supporting structures of mandibular second molars restored with different crown materials: 3-D finite element analysis (FEA). Journal of Prosthodontics. 2015; 24: 484–493.
[17] Cepic LZ, Frank M, Reisinger AG, Sagl B, Pahr DH, Zechner W, *et al.* Experimental validation of a micro-CT finite element model of a human cadaveric mandible rehabilitated with short-implant-supported partial dentures. Journal of the Mechanical Behavior of Biomedical Materials. 2022; 126: 105033.
[18] Soares CJ, Versluis A, Valdivia A, Bicalho AA, Veríssimo C, Barreto BdCF, *et al.* Finite element analysis in dentistry-improving the quality of oral health care. In Moratal D (ed.) Moratal D finite element analysis—from biomedical applications to industrial developments Intech (pp. 25–56). IntechOpen: Rijeka, Croatia. 2012.
[19] Bakke M, Holm B, Jensen BL, Michler L, Møller E. Unilateral, isometric bite force in 8–68-year-old women and men related to occlusal factors. European Journal of Oral Sciences. 1990; 98: 149–158.
[20] De Jager N, Pallav P, Feilzer AJ. The apparent increase of the Young's modulus in thin cement layers. Dental Materials. 2004; 20: 457–462.
[21] Dejak B, Mlotkowski A, Romanowicz M. Strength estimation of different designs of ceramic inlays and onlays in molars based on the Tsai-Wu failure criterion. The Journal of Prosthetic Dentistry. 2007; 98: 89–100.
[22] Gurbuz T, Sengul F, Altun C. Finite element stress analysis of short-post core and over restorations prepared with different restorative materials. Dental Materials Journal. 2008; 27: 499–507.
[23] Ausiello P, Apicella A, Davidson CL. Effect of adhesive layer properties on stress distribution in composite restorations—a 3D finite element analysis. Dental Materials. 2002; 18: 295–303.
[24] Patil AT, Surath S, Sandhyarani B, Nikam PP, Kulkarni TR, Pursnani V. A study on stress distribution of different preformed crowns in deciduous mandibular second molar using finite element analysis. Journal of Coastal Life Medicine. 2023; 11: 2289–2300.
[25] Guler MS, Guler C, Belduz Kara N, Odabasi D, Bekci ML. The stress distribution of a primary molar tooth restored with stainless steel crown using different luting cements. BMC Oral Health. 2024; 24: 269.
[26] Lath T, Rathi N, Mehta V, Mopagar VP, Patil RU, Hugar S, *et al.* Evaluation of stress generation in core build up-material of mutilated primary teeth: a comparative finite element analysis between BioFlx, stainless steel and zirconia crowns. Journal of Clinical Pediatric Dentistry. 2024; 48: 117–122.
[27] Doğan Ö. Stress distribution of pediatric zirconia and stainless steel crowns after pulpotomy procedure under vertical loading: a patient-specific finite element analysis. Journal of Functional Biomaterials. 2024; 15: 268.
[28] Oladapo BI, Zahedi SA, Vahidnia F, Ikumapayi O, Farooq MU. Three-dimensional finite element analysis of a porcelain crowned tooth. Beni-Suef University Journal of Basic and Applied Sciences. 2018; 7: 461–464.
[29] Deolikar S, Rathi N, Mehta V. Comparative evaluation of stress generation in primary teeth restored with zirconia and BioFlx crowns: a finite element analysis. Dental Journal. 2024; 57: 80–86.
[30] Hill EE. Dental cements for definitive luting: a review and practical clinical considerations. Dental Clinics of North America. 2007; 51: 643–658.
[31] Lagarde M, Francois P, Le Goff S, Attal JP, Dursun E. Structural and long-term mechanical properties from a resin-modified glass ionomer cement after various delays of light-activation. Dental Materials Journal. 2018; 37: 874–879.
[32] Güney Çildan B. Comparative evaluation of zirconia pediatric crowns and stainless steel crowns in primary teeth using finite element stress analysis [Specialization thesis]. Konya: Necmettin Erbakan University. 2019.
[33] Liu B, Lu C, Wu Y, Zhang X, Arola D, Zhang D. The effects of adhesive type and thickness on stress distribution in molars restored with all-ceramic crowns. Journal of Prosthodontics. 2011; 20: 35–44.
[34] Prabhakar AR, Chakraborty A, Nadig B, Yavagal C. Finite element stress analysis of restored primary teeth: a comparative evaluation between stainless steel crowns and preformed zirconia crowns. International Journal of Oral Health Sciences. 2017; 7: 10–15.
[35] Kindelan S, Day P, Nichol R, Willmott N, Fayle S. UK national clinical guidelines in paediatric dentistry: stainless steel preformed crowns for primary molars. International Journal of Paediatric Dentistry. 2008; 18: 20–28.
[36] Sajjanshetty S, Patil P, Hugar D, Rajkumar K. Pediatric preformed metal crowns—an update. Journal of Dental and Allied Sciences. 2013; 2: 29.
[37] Fonseca RB, Fernandes-Neto AJ, Correr-Sobrinho L, Soares CJ. The influence of cavity preparation design on fracture strength and mode of fracture of laboratory-processed composite resin restorations. The Journal of Prosthetic Dentistry. 2007; 98: 277–284.
[38] Yamanel K, Çaglar A, Gülsahi K, Özden UA. Effects of different ceramic and composite materials on stress distribution in inlay and onlay cavities: 3-D finite element analysis. Dental Materials Journal. 2009; 28: 661–670.
[39] Tanaka M, Naito T, Yokota M, Kohno M. Finite element analysis of the possible mechanism of cervical lesion formation by occlusal force. Journal of Oral Rehabilitation. 2003; 30: 60–67.
[40] Assunção WG, Barão VAR, Tabata LF, Gomes ÉA, Delben JA, dos Santos PH. Biomechanics studies in dentistry: bioengineering applied in oral implantology. Journal of Craniofacial Surgery. 2009; 20: 1173–1177.
[41] El-Anwar MI, Yousief SA, Soliman TA, Saleh MM, Omar WS. A finite element study on stress distribution of two different attachment designs under implant supported overdenture. The Saudi Dental Journal. 2015; 27: 201–207.
[42] Papazoglou AS, Karagiannidis E, Liatsos A, Bompoti A, Moysidis DV, Arvanitidis C, *et al.* Volumetric tissue imaging of surgical tissue specimens using micro-computed tomography: an emerging digital pathology modality for nondestructive, slide-free microscopy—clinical applications of digital pathology in 3 dimensions. American Journal of Clinical Pathology. 2023; 159: 242–254.
[43] Camargos GDV, Lazari-Carvalho PC, de Carvalho MA, Castro MB, Neris NW, Cury AADB. 3D finite element model based on CT images of tooth: a simplified method of modeling. Brazilian Journal of Oral Sciences. 2020; 19: e208910.

How to cite this article: Merve Taşcı Dedeoğlu, Merve Abaklı İnci. Evaluation of the biomechanical effects of pediatric crowns applied to endodontically treated primary molars: a three-dimensional finite element analysis. Journal of Clinical Pediatric Dentistry. 2026; 50(3): 187-198. doi: 10.22514/jocpd.2026.074.